IOP Publishing Smart Materials and Structures
Smart Mater. Struct. **25** (2016) 125015 (8pp) doi:10.1088/0964-1726/25/12/125015

High performance of macro-flexible piezoelectric energy harvester using a 0.3PIN-0.4Pb($Mg_{1/3}Nb_{2/3}$)O_3-0.3$PbTiO_3$ flake array

Zhou Zeng[1,3,4], Rongyu Xia[2], Linlin Gai[1,3], Xian Wang[1], Di Lin[1], Haosu Luo[1,4], Faxin Li[2,4] and Dong Wang[1]

[1] Key Laboratory of Inorganic Functional Material and Device, Shanghai Institute of Ceramics, Chinese Academy of Sciences, Shanghai 201800, People's Republic of China
[2] State Key Lab for Turbulence and Complex Systems, College of Engineering, Peking University, Beijing 100871, People's Republic of China
[3] University of Chinese Academy of Sciences, Beijing, 100049, People's Republic of China

E-mail: zengzhou@student.sic.ac.cn, hsluo@mail.sic.ac.cn and lifaxin@pku.edu.cn

Received 2 July 2016, revised 20 September 2016
Accepted for publication 30 September 2016
Published 11 November 2016

Abstract

Harvesting energy from human motion to power wearable devices using flexible piezoelectric energy harvesters is becoming a hot research topic, since this approach could fix the charging problem related to batteries and would do no harm to the environment. Unlike nano-generators, which have a piezoelectric material thickness at the level of a few nm to a few μm, we present a high-performance macro-flexible piezoelectric energy harvester (MF-PEH) with a piezoelectric material thickness of 45 μm, based on a 0.3PIN-0.4PMN-0.3PT (PIMNT) long flake array with an optimized cut. The piezoelectric properties of (110)-oriented PIMNT were studied as a function of thickness and compared to those of 0.7Pb($Mg_{1/3}Nb_{2/3}$)O_3-0.3$PbTiO_3$ (PMNT). The electrical properties of this device under different strain and load resistances are studied systematically. The results of our experiment show that under a strain of 0.225%, the open-circuit voltage and short-circuit current of MF-PEH reach levels as high as 23.2 V and 0.105 mA (at an excitation frequency of 1.1 Hz), respectively, with a maximum electric output power of 245 μW across a piezoelectric materials area of 400 mm^2. We have also used the device to harvest mechanical energy from the motion of human knees and charge a battery successfully. Efficient conversion from mechanical energy to electric energy and large output power demonstrate that our MF-PEH is an important complement to flexible energy harvesters and a potential candidate as a self-powered source for wearable low-power electronics.

Keywords: macro-flexible energy harvester, 0.3PIN-0.4PMN-0.3PT flakes, high performance, self-powered, wearable low-power electronics

(Some figures may appear in colour only in the online journal)

1. Introduction

Wearable devices, such as smart bracelets and Bluetooth or RF communication devices, are undergoing dramatic development for corporate, medical, and military applications. These devices require periodic renewal of their power sources, since their batteries will inevitably be discharged and must be recharged from an external energy source. In particular, the dependence of these electronics on batteries may give rise to risks to outdoor users, and the waste batteries may

[4] Author to whom any correspondence should be addressed.

even cause pollution to the environment. Offering smaller size and lower power consumption, the 'self-powered' concept has been proposed, which involves scavenging energy from ambient sources to power these devices [1–4]. A feasible way to do this is by harvesting energy from the human body as a sustainable energy source, such as from the knees (which have an average mechanical power of 49.5 W when walking [5]), using flexible piezoelectric energy harvesters (also called nano-generators or NGs) [6–8]. Even though piezoelectric NGs provide remarkable potential for use as renewable energy resources, these technologies still show low efficiency in operating mW-level electronics because of their low output electric power (from the nW to μW level) [9–11].

Since the power density of NGs is proportional to figure of merit dg (where d is the piezoelectric strain constant and g is the piezoelectric voltage constant) for a quasi-static piezoelectric energy harvester (PEH) [12], research has focused on materials with high piezoelectric properties, among which the relaxor-based ferroelectric single crystal $(1-x)$PMN-xPT (or PMNT) has sparked huge interest for its applications in NGs [13]. It has an exceptional figure of merit d_{32} . g_{32} up to 99 347 $\times$ 10^{-15} W N^{-2}, which is almost 20 times higher than that of PVDF, 40 times higher than that of PZT, and 200 times higher than that of $BaTiO_3$ [14, 15]. However, the piezoelectric constant of PMNT single crystals will evidently decline as their thickness decreases to the μm level because of their internal coarse domain structure and the surface-clamped effect [16], which makes the generated electric energy hugely decline. Recently researchers have found that PMNT crystals with fine domain structure could be obtained through certain poling conditions, but the poor stability of these domain structures makes it hard to use them in energy harvesters [17, 18]. Among relaxor-based xPT single crystals, xPIN-yPMN-(1-x-y)PT (or PIMNT) crystals not only possess a comparable figure of merit to PMNT, but also have more stable piezoelectric properties for their large coercive field and fine domain size. These advantages make PIMNT an ideal candidate for flexible energy harvesting [16, 19].

Similarly, increasing the thickness of the piezoelectric materials in flexible energy harvesters is another efficient approach to improving the generated power, since the electric energy density is proportional to the thickness. However, it is inevitable that the flexibility of the energy harvesters is decreased and there is a risk of mechanical damage with increased thickness. Thus, the macro-flexible energy harvester (in which the thickness of the piezoelectric materials is much larger than a few μm) is hard to put into application.

In this article, we combine the two approaches above and present a 0.3PIN-0.4PMN-0.3PT (PIMNT) single-crystal based macro-flexible PEH (MF-PEH), as shown in figure 1. Long PIMNT flakes in an optimized cut of $\langle 001\rangle^L \times \langle 1\text{-}10\rangle^W \times \langle 110\rangle^t$ are successfully prepared, where a high piezoelectric constant d_{32} exists [14]. With a thickness of 45 μm and a large aspect ratio of 10, these long flakes can not only decrease the stiffness of PIMNT, but also decrease the mechanical damage risk caused by micro-crack propagation under large stress. In addition, 10 PIMNT flakes bonded onto an acrylonitrile-butadiene-styrene (ABS) substrate were connected in parallel with their length direction parallel to that of the ABS substrate, so that the device could transfer bending stress from the human body in an efficient way and generate large output power. With this special material and structure, this device is designed to give excellent performance with high electric output power and mechanical stability.

2. Device fabrication

A schematic illustration of the fabrication process of MF-PEH is shown in figure 1(a). A (110)-oriented PIMNT crystal was cut into a square block and bonded onto a flat glass wafer with wax, then thinned to a flake with a thickness of 45 μm using grinding and subsequent chemical mechanical polishing. It is worth noting that Au electrodes were deposited on both the top and bottom surfaces after each polishing procedure. The flakes were then diced into cuboid plates with their $\langle 001\rangle$ and $\langle 110\rangle$ crystallographic axes oriented in the length and thickness directions, where a higher electromechanical response d_{32} exists compared to $\langle 100\rangle^L \times \langle 010\rangle^W \times \langle 001\rangle^t$ cut PMNT plates [14, 20]. The as-prepared plates were then taken off the glass wafer by heating to the melt temperature of the wax, and polarized along their thickness directions. Finally, ten polarized plates, two thin film flexible circuit, and one ABS flexible substrate were bonded together using high-strength epoxy (West System resin 105 and curing agent 206) to form a macro-flexible energy harvester, with PIMNT long flakes electrically connecting in parallel. It is rather remarkable that the copper electrodes on the thin film flexible circuit are a little smaller than the PIMNT flakes, which could not only prevent contact between the upper and bottom electrodes, but also protect the PIMNT flakes from mechanical damage. Figure 1(b) shows a photograph of the device. Table 1 lists the parameters of the proposed energy harvester.

3. Experiment methods

In order to find the relationship between the piezoelectric properties and the thickness of the piezoelectric materials used in our device, (110)-oriented PIMNT samples with a size of $6^{\langle 001\rangle} \times 2^{\langle 1\text{–}10\rangle} \times (0.03\text{–}0.8)^{\langle 110\rangle}$ mm^3 were prepared. PMNT samples of the same size were also prepared for comparison. The piezoelectric coefficient d_{32} was measured with an impedance analyzer (Agilent 4294) using the resonance and anti-resonance methods.

Then we conducted an experiment to compare the electric output properties of long PIMNT and PMNT flakes under bending stress. Flakes with a size of $20^{\langle 001\rangle} \times 2^{\langle 1\text{–}10\rangle} \times 0.045^{\langle 110\rangle}$ mm^3 were prepared and bonded onto the top face of the beryllium copper (with a size of 70 $\times$ 15 $\times$ 1 mm^3). A universal testing machine (Shimadzu AGS-10kNX) was used to apply force on the copper in a three-point bending way (as shown in the inset of figure 2(c)), and the strain in the flake was monitored by a strain amplifier (Donghua University DH3841) and a system electrometer (Keithley 6514).

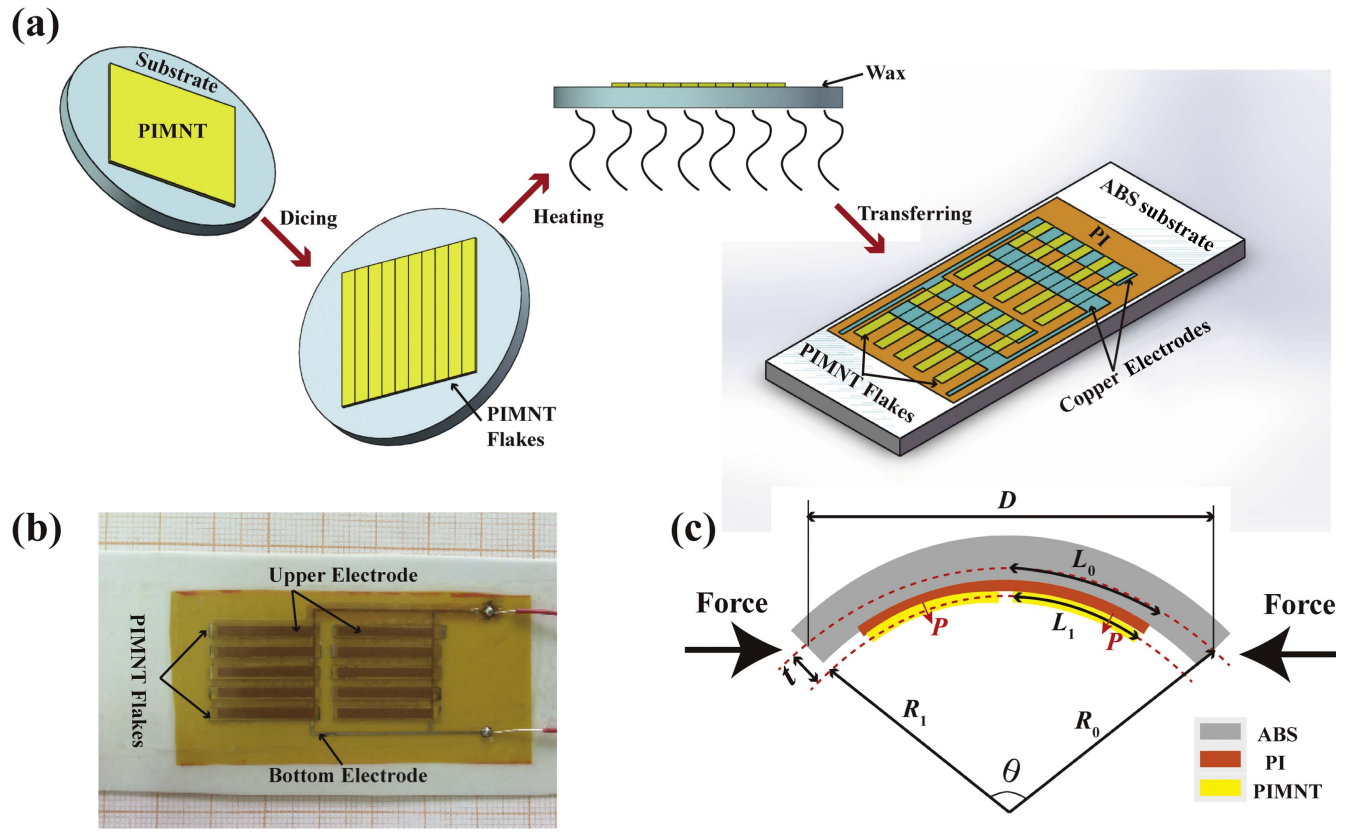

Figure 1. Schematic illustration of the fabrication process: (a) working principle schematic diagram and (b) photograph of (c) the macro-flexible 0.3PIN-0.4PMN-0.3PT PEH. The red line in (c) represents the poling direction in 0.3PIN-0.4PMN-0.3PT flakes. PI represents the kapton flexible circuit film; the copper electrodes are tightly bonded on the kapton film.

Table 1. Parameters of the proposed energy harvester.

Symbol	Value	Description
L	90 mm	Length of device (or ABS)
W	40 mm	Width of cantilever (or ABS)
t_A	0.22 mm	Thickness of ABS substrate
t_k	0.08 mm	Thickness of kapton film
W_k	30 mm	Width of kapton film
t_p	45 μm	Thickness of PIMNT flakes
w_P	2 mm	Width of PIMNT flakes
L_0	20 mm	Length of PIMNT flakes
E_k	1.5 Gpa	Young's modulus of ABS substrate
E_A	3 Gpa	Young's modulus of kapton film
E_{22}	58.8 Gpa	Transverse stiffness of PIMNT flakes (open circuit)
E'_{22}	14.5 Gpa	Transverse stiffness of PIMNT flakes (short circuit)
g_{32}	37.8 mV N^{-1}	Piezoelectric voltage constant of PIMNT flakes

The ferroelectric properties of PMNT and PIMNT were also tested to justify the difference between their piezoelectric performances. The domain configuration of poled PIMNT and PMNT were observed from the side view using a polarizing light microscope (Olympus BX-51), and ferroelectric *P–E* hysteresis loops of flakes with a thickness of 45 μm were measured by an analyzer (aixACCT TF-1000) at a frequency of 1 Hz.

As for examining the electric output properties of the MF-PEH, a linear motor was used to excite the device. The output voltage of the MF-PEH was monitored by a Tektronix Digital Oscilloscope (Agilent 54622A). For the open circuit, an impedance matching circuit which could avoid the impedance interference of the device was designed using a chip TL084CN (STMicroelectronics). During our experiments, various load resistances were used in order to characterize the performance of the device.

4. Theoretical analysis

In order to harvest the movement energy from human knees, we put the MF-PEH on the back of a tester's knees and fixed it with elastic strips. The device was forced to switching from the bending state to the unbending state periodically during walking or running, so that piezopotential was generated inside the PIMNT flakes. Figure 1(c) shows the working principle of our device. Assuming that the MF-PEH was bending to an angle of θ, then the strain ε induced in this device could be expressed as [21]:

$$\varepsilon = \frac{(L_1 - L_0)}{L_0} = \frac{(R_1 - R_0)}{R_0} = \frac{t}{R_0} = \frac{\theta t}{L} \qquad (1)$$

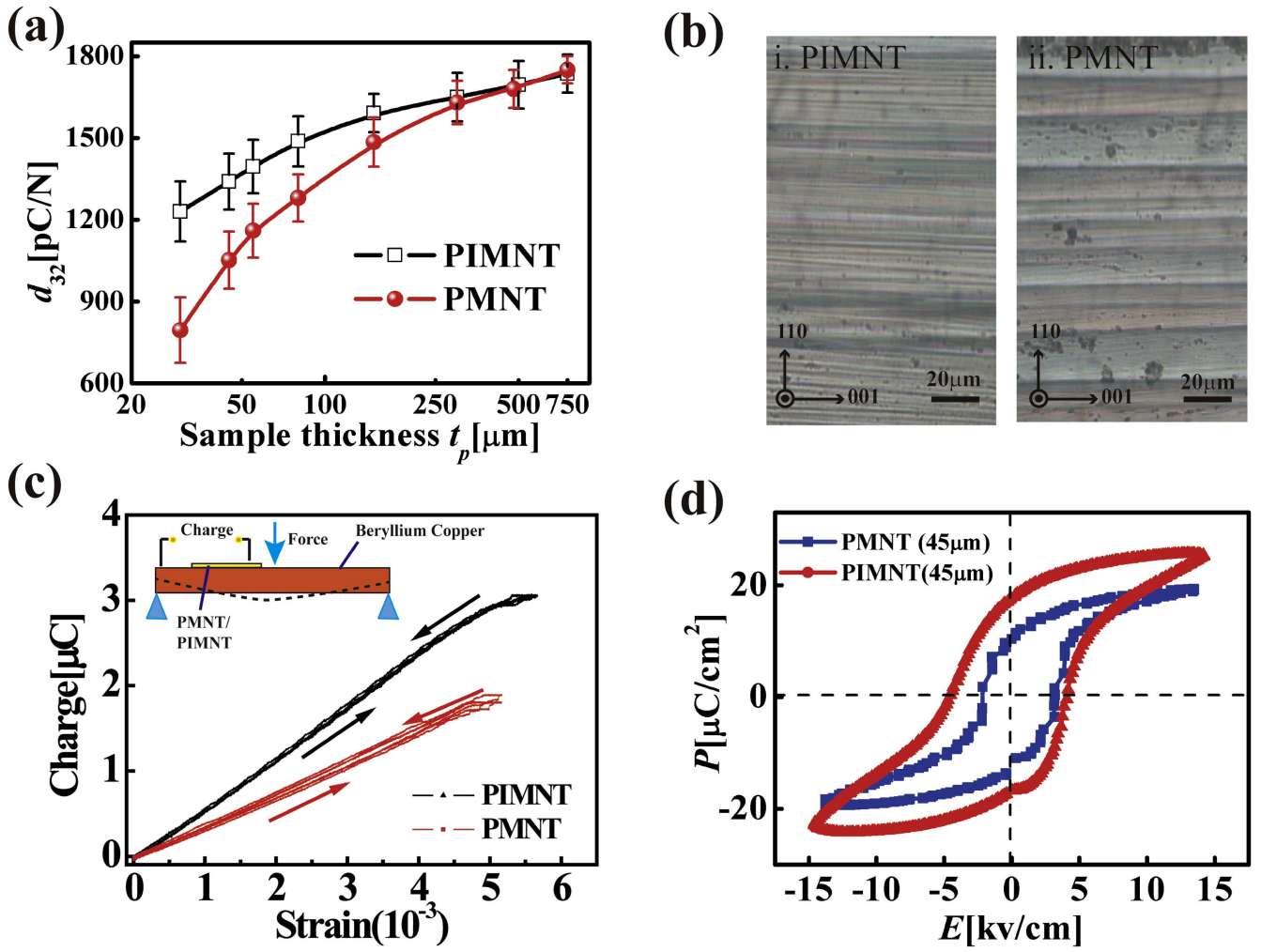

Figure 2. (a) The transverse piezoelectric constant d_{32} of PIMNT and PMNT single-crystal samples changes as a function of sample thickness; (b) domain configurations of PIMNT (i) and PMNT (ii) single crystals using polarized optical microscopes viewed from the side face (the poling direction is parallel to the ⟨110⟩ axis); (c) the generated charge in the PIMNT and PMNT flake as function of ac mechanical load. The inset shows a schematic illustration of the loading method; and (d) the hysteresis *P*–*E* loop of PIMNT and PMNT samples with a thickness of 45 μm.

where L_1 and L_0 are the length of the PIMNT in the compression (bending) state and origin state, respectively; L is the length of the whole device; R_1 and R_0 are the curvature radius of the neutral surface of the MF-PEH and the central plane of the PIMNT; and t is the distance between the neutral surface of the MF-PEH and the central plane of the PIMNT. As the thickness and surface area of the PIMNT flakes are much smaller than the ABS substrate and flexible circuit film, t approximately equals the distance between the neutral surface of the MF-PEH without PIMNT flakes and the top face of the kapton flexible circuit film. So t could be expressed as [22]:

$$t = \frac{\frac{1}{2}E_K W t_K^2 + \left(t_K + \frac{1}{2}t_A\right)E_A W_A t_A}{E_K W_K t_K + E_A W t_A}. \quad (2)$$

The angle θ could also be determined by the length of the MF-PEH in its original state and its span D in the bending state:

$$R_0 \sin\theta = D$$
$$R_0\theta = L. \quad (3)$$

The open-circuit voltage (OVC) of the piezoelectric macro-flexible energy harvester and the generated total charge Q at a short-circuit system can be theoretically described by [13]:

$$V = g_{32} \cdot \varepsilon \cdot E_{22} \cdot t_p \quad (4)$$

$$Q = d_{32} \cdot \varepsilon \cdot E'_{22} \cdot S \quad (5)$$

where S is the surface area of the piezoelectric material. Other details of the relative symbols in equations (2)–(5) are shown in table 1.

5. Results and discussion

Figure 2(a) shows that the transverse piezoelectric coefficient d_{32} of PIMNT and PMNT changes as a function of thickness.

As we can see, d_{32} in both the PIMNT and PMNT samples declines with the decrease in the sample thickness, especially when its thickness is less than 60 μm. It is the surface clamp effect that causes the deterioration of piezoelectric performance when the sample thickness decreases to the level of the domain size, as reported by Lee *et al* (2010) and Lin *et al* (2011) [16, 17, 19]. Figure 2(b) shows the domain structure of PMNT and PIMNT from the side view. PIMNT presents a finer domain size (<5 μm) than PIMNT (10–30 μm) after poling, which is why the d_{32} of PIMNT is more stable with a thickness decrease compared to that of PMNT. Figure 2(c) shows the charge generated in single PMNT and PIMNT flakes ($20 \times 2 \times 0.045\,\text{mm}^3$) as a function of ac mechanical load. Through a comparison of the slope in the linear region, we can see that the charge generated PIMNT flake is about 40% larger than PMNT at the same strain, which is consistent with figure 1(a) (the d_{32} of PIMNT is 37% larger than that of PMNT with a thickness of 45 μm). Besides, the PIMNT flake also presents a stable charge versus strain curve with a large linear region, while the PMNT flake shows an unstable curve with signs of a loop. It is likely that the domain or phase structure in PMNT was damaged under the large ac mechanical load. Figure 2(d) shows the ferroelectric *P*–*E* loop of PIMNT and PMNT flakes with a thickness of 45 μm. PIMNT presents a much larger coercive electric field compared to PMNT, which is why PIMNT flakes are more stable when undergoing a large mechanical load. These results prove that PIMNT is more stable and efficient than PMNT when used as a flexible energy harvester because of its fine domain structure and large coercive electric field.

Periodic bending/unbending motions of the MF-PEH were performed by a linear motor at a frequency of 1.1 Hz (approximately human walking frequency) to investigate the electric output of the harvesting device. Figure 3(a) shows a photograph of the MF-PEH driven by a linear motor. We set different amplitudes of step displacement ($A = L - D$) so that the maximum strain in the PIMNT could be controlled. With A varying from 2 mm ($\varepsilon = 0.112\%$) to 8 mm ($\varepsilon = 0.225\%$), the peak open-circuit voltage generated in the MF-PEH increased from 12.3 V to 23.2 V, as shown in figure 3(b). However, the measured piezopotential of the MF-PEH (12.3 V, 19.4 V and 23.2 V) is much lower than the theoretical values (112 V, 177 V and 225 V) calculated by equation (4). This deviation is presumably due to the voltage drop caused by uneven stress transformation from ABS to PIMNT (i.e., the strain induced on the location of the PIMNT flakes is smaller than the calculated one, while the strain induced elsewhere is larger than theoretical value) and internal charge loss. Figure 3(c) presents the output voltage and current on various load resistances from 10 Ω to 100 MΩ with A set at 8 mm. The peak short-circuit current was interpreted to be 105 μA across the piezoelectric materials area of $400\,\text{mm}^2$ ($10 \times 2 \times 20$ mm) using the epitaxial method. The electric output power of this device under different load resistances R_L is also presented in figure 3(d). The instantaneous power was calculated using the formula $P = U^2/R_L$, where U is the output peak voltage. As we can see, the maximum output power is about 245 μW at the match load resistance (about 500 kΩ), which is almost 1.5 times that in NGs based on the PMNT thick film energy harvester reported by Hwang *et al* [13]. These experiments demonstrate that the stability of piezoelectric properties in PIMNT flakes and relatively larger thickness contribute to the large output power of the MF-PEH to a large extent. A bending stability test was also conducted to confirm the mechanical robustness and durability of the harvester. Figure 3(e) shows that the OVC was measured consistently during 60 000 continual bending cycles of the device without noticeable degradation at maximum strain of 0.177% ($A = 4$ mm, $\theta = 59.6°$). This appears to be attributable to the stable piezoelectric properties of PIMNT under significant strain and specific structures of MF-PEH (i.e., a long flake array to decrease mechanical damage risk and protection from a flexible thin film circuit or ABS substrate).

In order to utilize the exceptional output power of our device as an additional energy source of commercial electronic devices, it is necessary to obtain high electric power from the mechanical movement of human joints. We put the MF-PEH on the back of a tester's knees and fixed it with elastic strips, as shown in figure 4(a)(i). Figure 4(a)(ii) shows an analysis of the strain induced in PIMNT flakes when moving. The amplitude of the angle between thigh and calf is about 60°–70° during normal walking or running [23], and thus the theoretical maximum strain induced in PIMNT is about 0.16%–0.186% calculated by equation (1). In the case of human walking or running, an electric signal will be generated and transferred to the electronic devices. Figure 4(b) shows that the OVC increases from 0 V to 12.3 V and 15.9 V as we change our movement from standing to walking (with a frequency of about 1.1 Hz) and running (with a frequency of about 2.3 Hz). These experimental results are slightly lower than the results in figure 4(b) since the theoretical maximum strain of 0.16%–0.186% is close to 0.177% (with OVC of 19.4 V). The main reason for this phenomenon may lie in the fact that the MF-PEH is not closely fitted to the back of the knee. Forty-eight parallel and serial-connected blue LEDs were lit simultaneously with the generated electric power from the momentary bending and unbending motions of the MF-PEH during running, as shown in the inset. Figure 4(c) shows that a coin cell (Sanyo ML414) was charged by the continual bending and unbending of the MF-PEH in different movement states (from 0.03 V to 1.8 V for walking and from 0.03 V to 2.45 V for running in 1 h, respectively) and the inset depicts the equivalent circuit diagram of the connection for energy storage (AC signals were therefore converted into DC signals using a full-wave bridge-rectification circuit composed of four diodes). The large output power generated in these experiments indicates that MF-PEH could be used as a potential new energy source for smart wearable devices, such as watches, LED screens and Bluetooth devices, thereby resolving intrinsic issues such as increment of battery size or replacement of discharged batteries.

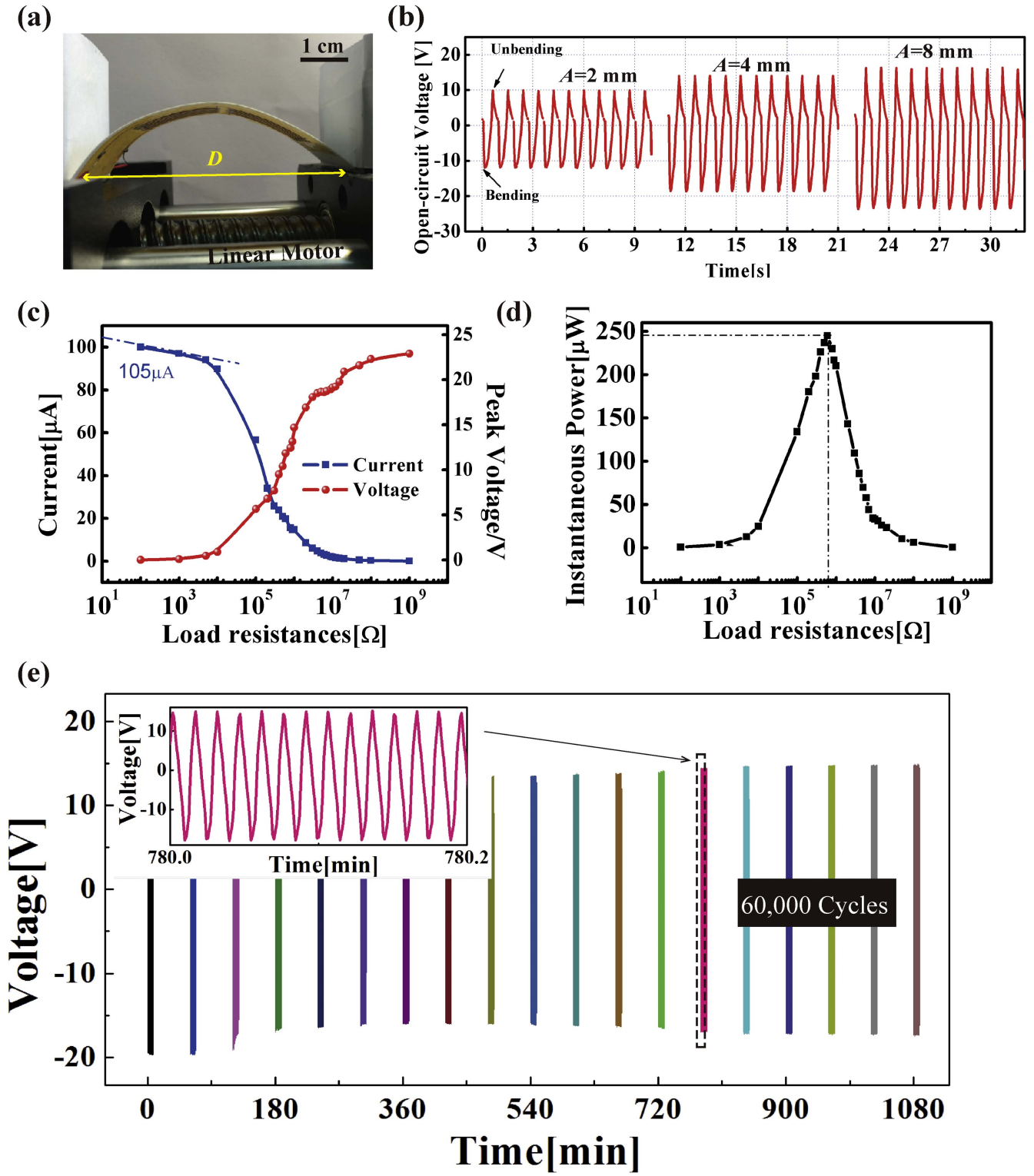

Figure 3. (a) Optical images of the MF-PEH in the bending state for power generation; (b) the open-circuit voltage signals generated from the proposed energy harvester at strain of 0.112% (A = 2 mm, θ = 42.1°), 0.177% (A = 4 mm, θ = 59.6°) and 0.225% (A = 8 mm, θ = 84.8°) at an excitation frequency of 1.1 Hz; the measured output voltage and current (c) and the instantaneous electric power (d) of the MF-PEH under different load resistances varying from 10 Ω to 100 MΩ at 1.1 Hz (a maximum instantaneous power of 0.245 mW is obtained at 500 kΩ); (e) the result of continuous bending fatigue tests up to 60 000 iterations to confirm the mechanical durability of MF-PEH and a zoomed view of the black dotted region (inset). The data were measured every 60 min with a duration of 500 s.

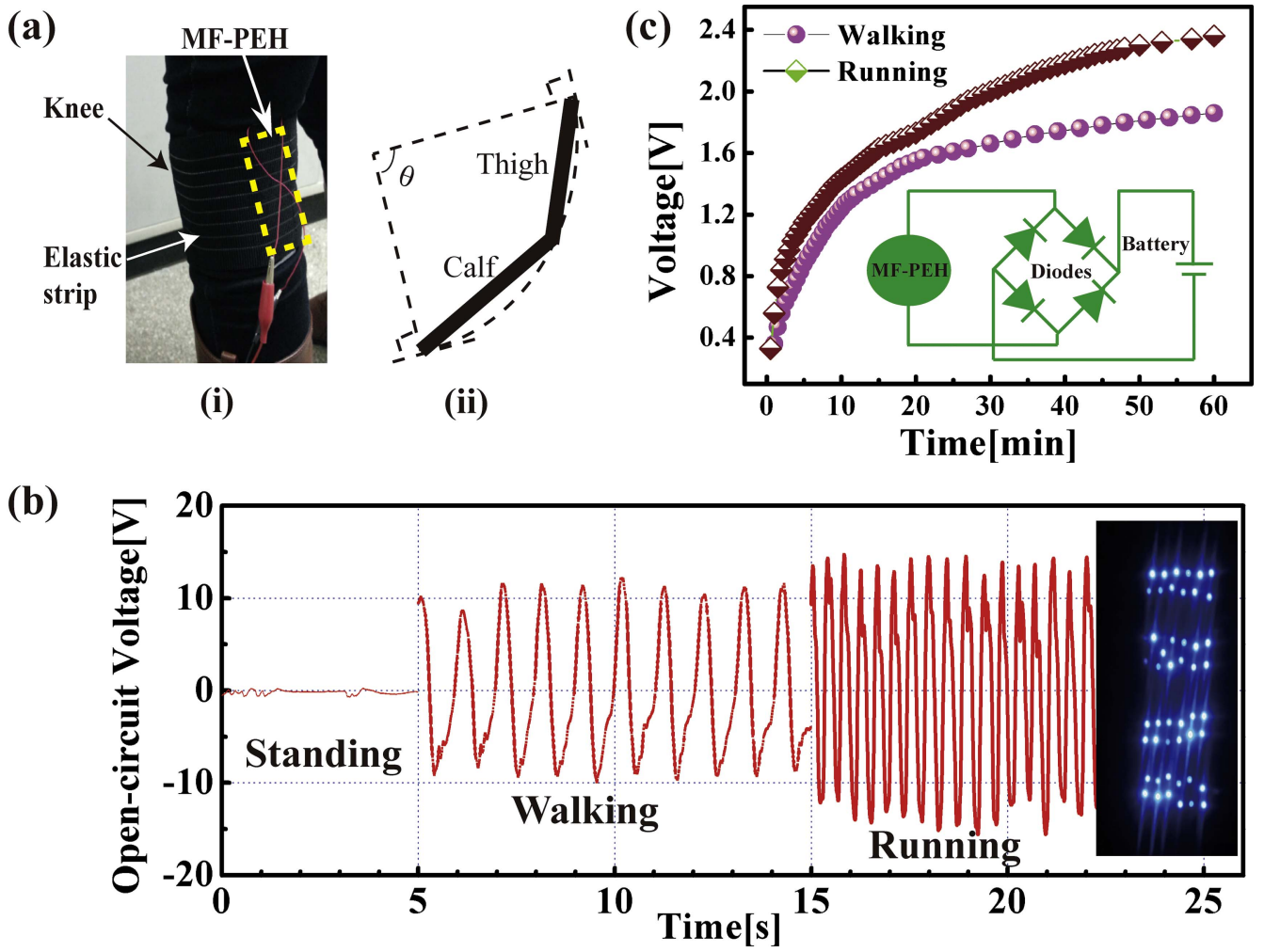

Figure 4. (a) A photograph (i) and a schematic illustration of the bending deformation (ii) of the MF-PEH when put on the back of a tester's knees; (b) the measured open-circuit voltage of the MF-PEH under normal human walking and running motions (the graph in the inset shows that 48 hybrid-connected blue LEDs were lit by this device when running); (c) the charge curve of a chargeable lithium battery (Sanyo ML414) when serially connected to the MF-PEH under different movement states (the inset depicts the equivalent circuit diagram of the connection for energy storage).

6. Conclusion

In summary, a high-performance macro-flexible energy harvester based on an array of 0.3PIN-0.4PMN-0.3PT single-crystal flakes was successfully prepared. The piezoelectric charge constant d_{32} of PIMNT changes as a function of thickness was studied and compared to that of PMNT. Our experimental results show that PIMNT is more stable in piezoelectric properties with decreasing thickness and presents much higher d_{32} in flakes (especially when thickness is below 60 μm) because of its large coercive field and fine domain size. Thus, PIMNT flakes are more efficient than PMNT when used in flexible energy harvesters. In addition, the electric output properties of the MF-PEH was studied using a linear motor. The maximum OVC and extrapolation current of the proposed device reached as high as 23.2 V and 0.105 mA with a strain of 0.225%, respectively. The instantaneous electric power reached as high as 245 μW under a matching load resistance of 500 kΩ. Finally, the PIMNT based MF-PEH was put on the back of a tester's knees to convert mechanical energy into electric energy as a sustainable energy source for electronic devices. Because of the high output power, 48 blue LEDs could be lit during running, and a rechargeable battery (Sanyo ML414) was charged to 2.45 V after 1 h of running. We believe that with a high-efficiency electrical power management circuit, the MF-PEH is a potential candidate as a self-powered source for both military and commercial wearable low-power electronics.

Acknowledgments

This work was financially supported by the Ministry of Science and Technology of China through the 973 Program (grant no. 2013CB632900), the Natural Science Foundation of China (grant nos 51332009, 51272268 and 15DZ2251200) and the Shanghai Natural Science Foundation (no. 15ZR1419400).

References

[1] Qin Y, Wang X and Wang Z L 2008 Microfibre-nanowire hybrid structure for energy scavenging *Nature* **451** 809

[2] Wu L, Yuan W, Hu N, Wang Z, Chen C, Qiu J, Ying J and Li Y 2014 Improved piezoelectricity of PVDF-HFP/carbon black composite films *J. Phys. D: Appl. Phys.* **47** 135302

[3] Su Y, Xie G, Xie T, Zhang H, Ye Z, Jing Q, Tai H, Du X and Jiang Y 2016 Wind energy harvesting and self-powered flow rate sensor enabled by contact electrification *J. Phys. D: Appl. Phys.* **49** 215601

[4] Hwang G-T *et al* 2015 A reconfigurable rectified flexible energy harvester via solid-state single crystal grown PMN-PZT *Adv. Energy Mater.* **5** 1500051

[5] Niu P, Chapman P, Riemer R and Zhang X D 2004 Evaluation of motions and actuation methods for biomechanical energy harvesting *35th Annual IEEE Power Electronics Specialists Conf. (PESC 2004). Aachen, Germany.* pp 2100–6

[6] Jeong C K *et al* 2015 A hyper-stretchable elastic-composite energy harvester *Adv. Mater.* **27** 2866–75

[7] Park K-I *et al* 2012 Flexible nanocomposite generator made of $BaTiO_3$ nanoparticles and graphitic carbons *Adv. Mater.* **24** 2999–3004

[8] Delnavaz A and Voix J 2014 Flexible piezoelectric energy harvesting from jaw movements *Smart Mater. Struct.* **23** 105020

[9] Chung S Y, Kim S, Lee J-H, Kim K, Kim S-W, Kang C-Y, Yoon S-J and Kim Y S 2012 All-solution-processed flexible thin film piezoelectric nanogenerator *Adv. Mater.* **24** 6022–7

[10] Lee J-H *et al* 2014 Highly stretchable piezoelectric–pyroelectric hybrid nanogenerator *Adv. Mater.* **26** 765–9

[11] Zhang H *et al* 2015 A flexible and implantable piezoelectric generator harvesting energy from the pulsation of ascending aorta: *in vitro* and *in vivo* studies *Nano Energy* **12** 296–304

[12] Priya S 2007 Advances in energy harvesting using low profile piezoelectric transducers *J. Electroceram.* **19** 165–82

[13] Hwang G-T *et al* 2014 Self-powered cardiac pacemaker enabled by flexible single crystalline PMN-PT piezoelectric energy harvester *Adv. Mater.* **26** 4880–7

[14] Wang F, Luo L, Zhou D, Zhao X and Luo H 2007 Complete set of elastic, dielectric, and piezoelectric constants of orthorhombic $0.71Pb(Mg_{1/3}Nb_{2/3})O_3$-$0.29PbTiO_3$ single crystal *Appl. Phys. Lett.* **90** 212903

[15] Beeby S P, Tudor M J and White N M 2006 Energy harvesting vibration sources for microsystems applications *Meas. Sci. Technol.* **17** R175–95

[16] Lee H, Zhang S, Luo J, Li F and Shrout T R 2010 Thickness-dependent properties of relaxor-$PbTiO_3$ ferroelectrics for ultrasonic transducers *Adv. Funct. Mater.* **20** 3154–62

[17] Lin D, Lee H J, Zhang S, Li F, Li Z, Xu Z and Shrout T R 2011 Influence of domain size on the scaling effects in Pb(Mg1/3Nb2/3)O-3-$PbTiO_3$ ferroelectric crystals *Scr. Mater.* **64** 1149–51

[18] Wada S, Yako K, Kakemoto H, Tsurumi T and Kiguchi T 2005 Enhanced piezoelectric properties of barium titanate single crystals with different engineered-domain sizes *J. Appl. Phys.* **98** 014109

[19] Lee H J, Zhang S and Shrout T R 2010 Scaling effects of relaxor-$PbTiO_3$ crystals and composites for high frequency ultrasound *J. Appl. Phys.* **107** 124107

[20] Zhou D, Wang F, Luo L, Chen J, Ge W, Zhao X and Luo H 2008 Characterization of complete electromechanical constants of rhombohedral $0.72Pb(Mg_{1/3}Nb_{2/3})$-$0.28PbTiO_3$ single crystals *J. Phys. D: Appl. Phys.* **41** 185402

[21] Park K-I, Xu S, Liu Y, Hwang G-T, Kang S-J L, Wang Z L and Lee K J 2010 Piezoelectric $BaTiO_3$ thin film nanogenerator on plastic substrates *Nano Lett.* **10** 4939–43

[22] Mateu L and Moll F 2005 Optimum piezoelectric bending beam structures for energy harvesting using shoe inserts *J. Intell. Mater. Syst. Struct.* **16** 835–45

[23] Li Q, Naing V and Donelan J M 2009 Development of a biomechanical energy harvester *J. Neuroeng. Rehabil.* **6** 22